SINTERING AND EXPANSION OF HTSC CERAMICS

H.M. O'BRYAN

AT&T Bell Laboratories, Murray Hill, NJ 07974 (U.S.A.)

(Received 29 January 1990)

ABSTRACT

The sintering and processing of superconductors based on Ba–Y–Cu oxides and Bi–Sr–Ca–Cu oxides are briefly reviewed. The expansion behaviors of the above materials and the Pr–Sr–(YCa)–Cu oxides are discussed. It is shown that expansions can be separated into compositional and thermal contributions. Published data through August 1989 are included in this review.

INTRODUCTION

The need for dense, single phase ceramics of the copper-based superconductor became apparent once the research emphasis shifted from critical temperature toward engineering properties. It was obvious that an efficient conductor must avoid large inclusions, be they voids, second phases in the bulk or at grain boundaries and regions of off-stoichiometry. The translation of these needs into materials has been the task of the materials processing engineer. This article will review their success with reference to the sintering and densification of $Ba_2YCu_3O_7$ and BiSrCaCu oxides. Also included will be data, obtained by thermal analytical techniques, regarding the expansion of materials during heating for the above materials and $Pb_2Sr_2(YCa)Cu_3$ oxides.

Normally crystalline oxide ceramics are obtained by sintering precursor powders which have been obtained either by the decomposition of a solution or by solid state reaction of individual oxides. Prior to sintering, powders prepared from either precursor are prereacted so that the material to be sintered already contains a majority of the final compound. For chemically-prepared powders prereaction can often be accomplished at a lower temperature than that required for powder prepared by a solid state reaction. Thermal analysis of the individual and mixed raw materials as well as the prereacted powder are useful in identifying problem compounds or optimizing the conditions for sintering. In sintering densification occurs at some temperature below the melting point as individual particles grow and the

total porosity decreases under the driving force of a reduction of total surface energy. For high density the initial particle size should be small and the particles should not undergo a gas forming decomposition at the sintering temperature.

$Ba_2YCu_3O_x$ CERAMICS

The processing of $Ba_2YCu_3O_x$ (i.e. 1-2-3) into ceramic shapes utilizes techniques which have been developed for other oxide materials. Such operations as mixing, prereaction, grinding, forming and sintering utilize the same principles for oxide superconductors as those applied to processing ferrites, piezoelectric, substrate and package materials. Processing of 1-2-3 material, however, also entails some unusual problems [1,2]. Three of these concern decomposition of $BaCO_3$, reaction with water and reoxidation annealing. These will be discussed at the appropriate step in the processing sequence.

To prepare a suitable powder for sintering, carefully weighed portions of $BaCO_3$, Y_2O_3 and CuO are thoroughly mixed and then prereacted at 850°C to 900°C in air or oxygen. In handling large amounts of powder, wet mixing in water using a high speed blender, a ball mill or a muller mixer is convenient. When wet mixing is used, it is important that the liquid removal does not produce segregation of the constituents. If a slurry is allowed to settle during filtration, evaporation, spray drying or decantation, segregation of the oxides/carbonates can occur. Table 1 shows the composition variation across a filter cake which formed as the liquid was removed from a slurry of $BaCO_3$, Y_2O_3 and CuO. When material with such non-uniformity is

TABLE 1

Phase amounts in various sections of filter cake from mixed raw materials

Filter cake	Y_2O_3	CuO	$BaCO_3$	$BaCuO_2$	$Ba_3YCu_2O_x$	Y_2BaCuO_5	$Ba_2YCu_3O_x$
Unreacted (normalized to 100 for $BaCO_3$)							
Top (glaze)	19 [a]	20	100				
2nd (dark)	23	14	100				
3rd (light)	25	44	100				
4th (dark)	170	260	100				
Granulated	44	30	100				
Prereacted 900 °C/24 h/O_2 (normalized to 100 for phase of highest concentration)							
Top		–		20	100	–	50
Bottom		100		–	–	50	35
Granulated		52		13	84	66	100

[a] Relative intensity of major peaks.

prereacted, the compounds $Ba_3YCu_2O_x$, CuO or Y_2BaCuO_5 will predominate where different constituents have concentrated. Uniformity in microstructure and composition is very difficult to obtain in the sintered ceramic once such segregation has occurred.

At the prereaction temperature of $900\,°C$ $BaCO_3$ decomposition is slow, and long prereaction times or multiple prereactions with regrinding are required to eliminate the $BaCO_3$. Higher temperatures for prereaction are to be avoided because of the increased particle size. Even when no $BaCO_3$ is observed, BaO may be present and it can reabsorb CO_2 or take up H_2O. The presence of compounds which form a gas during decomposition interferes with sintering, as will be shown.

Once the raw materials have reacted to form 1-2-3, reaction with normal atmospheres is negligible and prereacted powders show no change in phase distribution after 2 years of storage. This is not the case where water or $85\,°C/85\%$ relative humidity is present. In either environment, decomposition of the reacted powder is very rapid and indeed decomposition also occurs at a slower rate with sintered ceramics. Hence, the wet grinding of the prereacted powders must be performed under an organic liquid and the 1-2-3 ceramic must be protected from water in any application.

Sintering of pressed compacts occurs at $950\,°C$ to $975\,°C$ in O_2. To prevent the inclusion of gas from the decomposition of either hydroxides or carbonate, the sintering schedule often uses a slow heating rate near $900\,°C$ to permit any gas to dissipate before the pore structure becomes closed. Figure 1 shows the porosity which occurs during the sintering of powder containing unreacted $BaCO_3$. In powders produced by a solid state reaction, agglomerates in the powder can produce inhomogeneities in density. A slight CuO excess generates a liquid which yields more homogeneous and denser microstructures. The effect of small deviations in cation composition from the 1-2-3 values has been examined in a careful study which found density differences of 71% to 97% with high densities obtained for Cu-rich compositions [2]. Accompanying the higher density was a larger grain size. Several alternatives to sintering, such as melt-texture growth [3], glass devitrification [4], and hot pressing/hot forging [5] have been used to obtain microstructures with special grain arrangements.

For $Ba_2YCu_3O_x$ ceramic the equilibrium oxygen stoichiometry is $x \approx 6.2$ at $900\,°C$ in 1 atm oxygen. To obtain a $T_c > 90$ K the oxygen content must be raised to $x \approx 6.98$ by a low temperature anneal. The difficulty of transporting oxygen through a dense ceramic has not always been appreciated [23]. For a dense ceramic, full oxidation requires oxygen to diffuse along grain boundaries and across grains which already have values of $x \approx 7$. The result is a decreasing rate of oxidation with time, as long as the specific volume of the oxidized layer remains greater than or equal to that of the unoxidized ceramic. For 1-2-3 the specific volume changes greatly with temperature and a protective layer is only possible for oxidation above
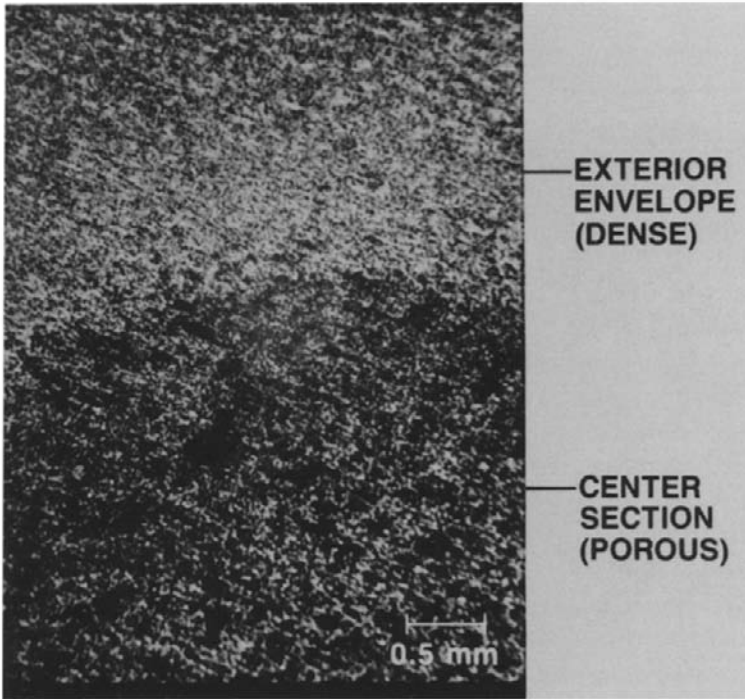
Fig. 1. Interior section of a $Ba_2YCu_3O_x$ ceramic sintered at 950 °C in oxygen. Pressed powder contained $BaCO_3$ which decomposed during sintering to produce a porous center section.

600 °C. Figures 2 and 3 show this effect, as parabolic kinetics are observed when the protective layer is maintained at temperatures greater than 500 °C while linear oxidation is observed at 500 °C or below where cracks in the oxidized layer allow oxygen transport via the gas phase. The intact thin layer
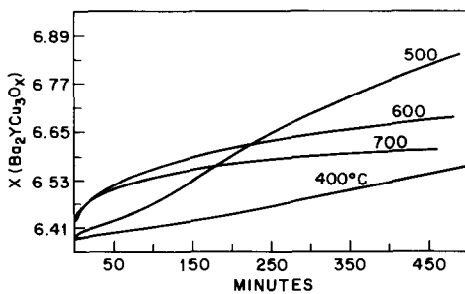

Fig. 2. Kinetics of oxidation for $Ba_2YCu_3O_{6.37}$ ceramic. Initial density is 6.0 g cm^{-3} [23].
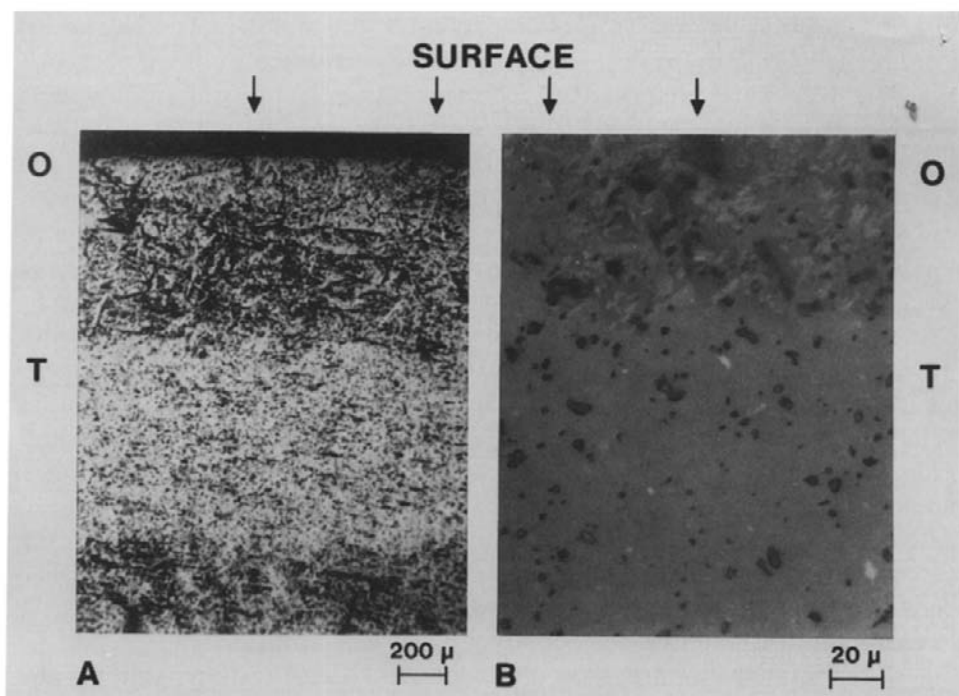
Fig. 3. Microstructure of dense ceramic which has been partially oxidized at 500 °C (A) Thick oxidized layer (orthorhombic with high specific volume) near surface and (B) thin oxidized layer. Note that the thick layer has cracked extensively while the thin layer is still intact [23].

and cracked thick layer in Fig. 3 correspond to the initial oxidation region (parabolic) and later oxidation region (linear) of the 500 °C curve in Fig. 2.

BiSrCaCu OXIDES

The discovery by Maeda [6] that the rare-earth free BiSrCaCu oxide system produced compounds with attractively high T_c values initiated intense research activity on these materials. In this family, the presence of Bi required that the sintering temperature be reduced to avoid melting while the absence of Ba and rare earths suggested that higher temperatures might not be necessary to obtain complete reaction. Initially processing followed the same paths used successfully for 1-2-3. Well-mixed CuO, Bi_2O_3, $SrCO_3$ and $CaCO_3$ powder is prereacted at 800 °C in air. 2–10 h are sufficient to produce a powder whose X-ray pattern does not contain any trace of carbonates or unreacted CuO. Multiple grindings and prereactions are possible, but usually a single wet milling is sufficient to obtain homogeneity in the reacted powder. Since the powder does not decompose in water, milling is simplified. As noted previously, care must be taken to avoid

resegregation during processing. Compaction of the milled powder, however, is more difficult than for the 1-2-3 because the prereacted Bi based compositions are very soft and spring-like. Consequently, dry pressing often causes sticking at the die surfaces.

The major problem with the sintering of the Bi compound comes from the existence of at least three structurally related, chemically similar but electrically different layered cuprate compounds. They are described in terms of their number of CuO layers (as 1, 2 or 3) or in terms of their approximate T_c (as 20 K, 80 K or 107 K). The formation of these compounds is sensitive to cation stoichiometry and thermal history. Maeda found the presence of both the 80 K and 107 K compounds in a starting composition of $BiSrCaCu_2O_x$ (1112) heated at 880°C for 9 h in air. Although the approximate cation compositions for the 20 K, 80 K and 107 K compounds are 2201, 2212 and 2223 (Bi–Sr–Ca–Cu), it has become apparent that the predominant compound, formed during sintering, does not have the composition of the initial batch. Therefore most sintered materials are not single phased and the agreement between various investigations regarding phase distribution has been poor.

Generally the sintering temperatures have been from 840°C to 890°C, but little data are reported on the successful densification. Rather, the sintering is used more as a means of completing phase formation. Indeed, pressed powder compacts are observed to decrease in bulk density (increased dimension) as the sintering time is increased (Fig. 4) [7]. This phenomenon, known as retrograde sintering, is caused by anisotropic grain growth. As the flake-like grains become larger by adding material at their edge, the adjacent grains are pushed away. The resulting microstructure resembles a lacelike pattern and grains of diameter 100 μm and thickness less than 1 μm have been observed. Such ceramics have densities well below 3 g cm^{-3} while the
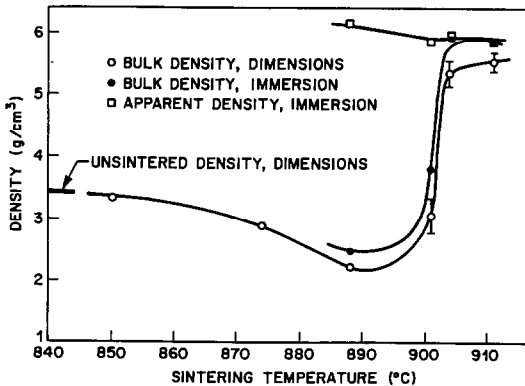

Fig. 4. Density of $Bi_2Sr_2CaCu_2O_8$ samples as a function of temperature after sintering for 2 h in oxygen.

theoretical density is near 7 g cm^{-3}. To achieve higher density the sintered ceramic may be crushed and resintered. A density increase from 2.0 g cm^{-3} to 3.5 g cm^{-3} has been obtained for Pb-doped Ba$_2$Sr$_2$Ca$_2$Cu$_3$O$_x$ which has been sintered, crushed and resintered [8]. Other schemes for increasing density involve grain alignment. By forcing the grains to lie with their major axes parallel, anisotropic growth can be made to assist pore removal rather than pore enlargement. One approach is to interrupt the sintering heat treatment in order to apply a uniaxial pressure [9]. Afterwards the sintering is continued with the grains now aligned with their major axes perpendicular
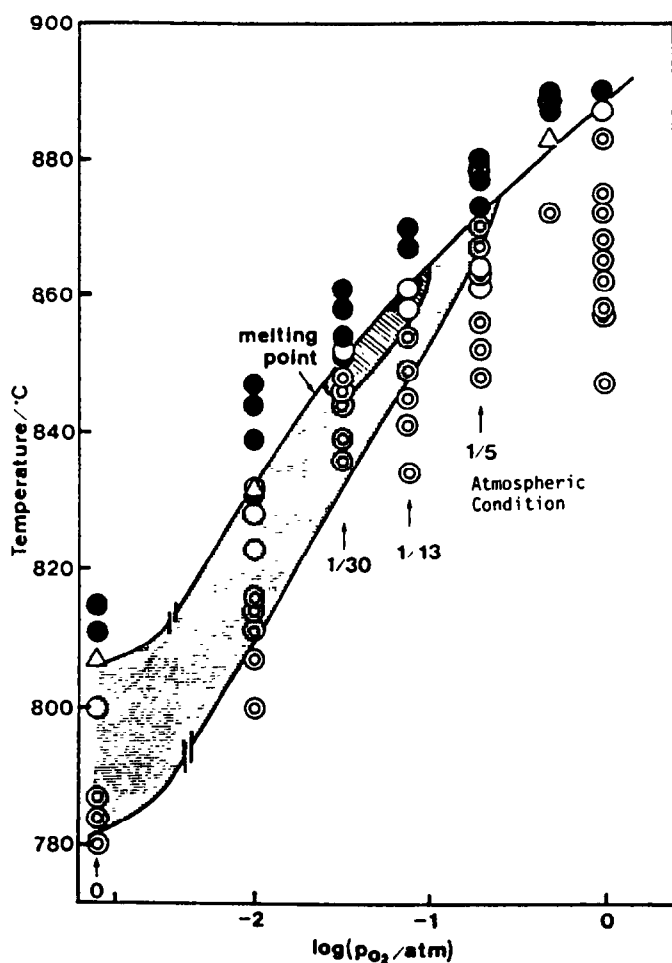
Fig. 5. Effect of oxygen pressure and reaction temperature on the formation of Bi$_1$Sr$_1$Ca$_1$Cu$_2$O$_y$ superconductors. ● indicates that the samples melted, Δ indicates partially melted, ○ indicates not melted through transformed and ⊙ indicates not melted at all. The high T_c phase appears in the dotted area and more preferably in the dashed area. The high T_c phase formation is most clear at the temperature just below the melting point under oxygen pressure of 1/13 atm [12].

to the pressing direction. Using this approach, a $7 \times$ improvement in J_c is obtained and the microstructure indicates considerable density improvement [10]. A second approach also uses a uniaxial pressure, applied during sintering to align grains, and a 6.2 g cm^{-3} density is reported [11].

As Fig. 4 shows, density is increased when the sintering temperature produces liquid formation. Like 1-2-3 the Bi compounds do not melt congruently. Therefore, it is possible to control the amount of liquid formed. It has been shown that for the 1112 composition p_{O_2} strongly influences the amount of liquid formation [12]. In Fig. 5 melting begins near 810°C for 10^{-3} atm of oxygen and at 885°C for 1 atm of oxygen. A major problem with enhancing densification by liquid phase sintering is that the 107 K phase does not form readily in melted samples and long anneals are required [13].

Processing innovations which are conducive to 107 K phase formation are PbO addition [14] and a long sintering time [15,16]. One often overlooked problem in sorting out the proper conditions for 107 K phase formation is the substantial effect that minute changes in oxygen stoichiometry (< 0.01% weight change) have on T_c [17–19]. Presently the preferred route for obtaining the 107 K phase ceramic is to substitute 20% PbO for Bi_2O_3, use a batch formulation rich in Ca and Cu, and sinter at P_{O_2} values of $\sim 10^{-1}$ atm near 850°C for extended periods. The resulting ceramics have a sharp T_c transition when measured by a.c. susceptibility, and are nearly single phase. Densities, however, remain very low.

COMPOSITIONAL AND THERMAL EXPANSION

Among the more important, and certainly one of the most interesting, groups of thermal analytical data, obtained for the HTSC, are their expansion behaviors. Normally polycrystalline materials show gradual reversible changes in length (during heating and cooling) as the lattice parameters respond to temperature. Crystallographic transformations will produce discontinuous length changes for a first order transition and a change in thermal expansion coefficient (CTE) for a second order transition. In these superconducting groups the strong dependence of the lattice volume on oxygen stoichiometry as well as the ease with which the compound can change its oxygen content combine to produce a reversible compositionally dependent expansion. Often such length changes are much larger than the thermal effects. Where the oxygen stoichiometry is able to change as a function of temperature, the compositional and thermal expansion effects become merged. Measurements of expansion have been obtained by dilatometry, high temperature XRD and high temperature neutron diffraction. Results for three HTSC families are discussed.
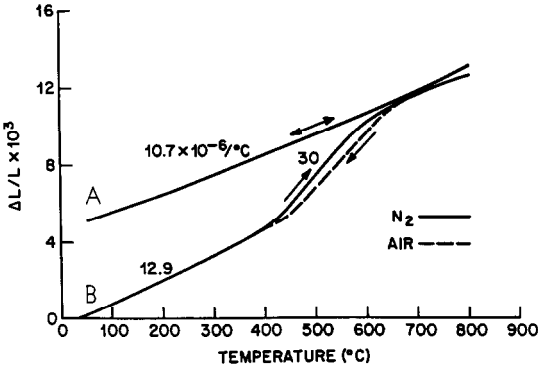
Fig. 6. Expansion of (A) $Ba_2YCu_3O_{6.2}$ in nitrogen and (B) $Ba_2YCu_3O_7$ in air. Measured with a dilatometer. Heating rate $4°C \ min^{-1}$.

$Ba_2YCu_3O_x$

The relative contributions of the compositional and thermal expansions in 1-2-3 can be estimated from the data in Fig. 6 [20,21]. When a sample with $x \approx 6.2$ is heated or cooled between 25°C and 800°C in a nitrogen atmosphere, there is a nearly constant expansion with a CTE of $10.7 \times 10^{-6} \ °C^{-1}$ [20,22]. By contrast, when a sample with $x \approx 7$ is heated in air, initially the CTE is $12.9 \times 10^{-6} \ °C^{-1}$ but a larger CTE is observed for the expansion between 450°C and 650°C [25]. This temperature region and atmosphere coincide with the conditions where 1-2-3 begins to lose oxygen and suggests a strong compositional component to expansion. Cooling in an oxidizing atmosphere produces a compositional shrinkage. This contribution can be isolated by isothermal dilatometry in different atmospheres (Fig. 7) [21]. The magnitudes of these length changes seem to suggest a compositionally-in-
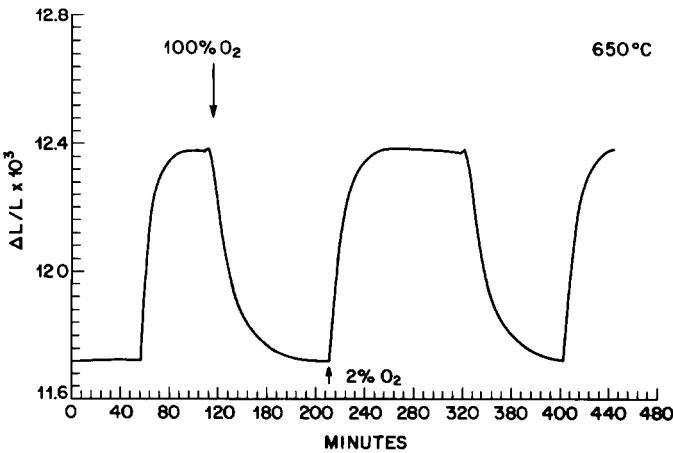

Fig. 7. Isothermal expansion of $Ba_2YCu_3O_x$ as the atmosphere is switched between 2% oxygen in nitrogen and oxygen. Measurements by mechanical dilatometry.
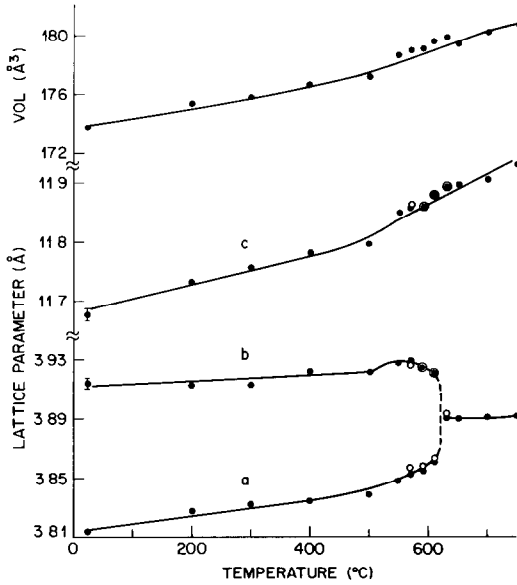
Fig. 8. Anisotropy of thermal expansion in air. Lattice parameter data obtained from HT-XRD. ●, Heating; ○, cooling.

duced phase charge, and indeed the $x = 7$ and $x = 6.2$ compositions have different crystal structures. However, high temperature XRD (Fig. 8) [20] and neutron diffraction [24] both show that the lattice parameter changes
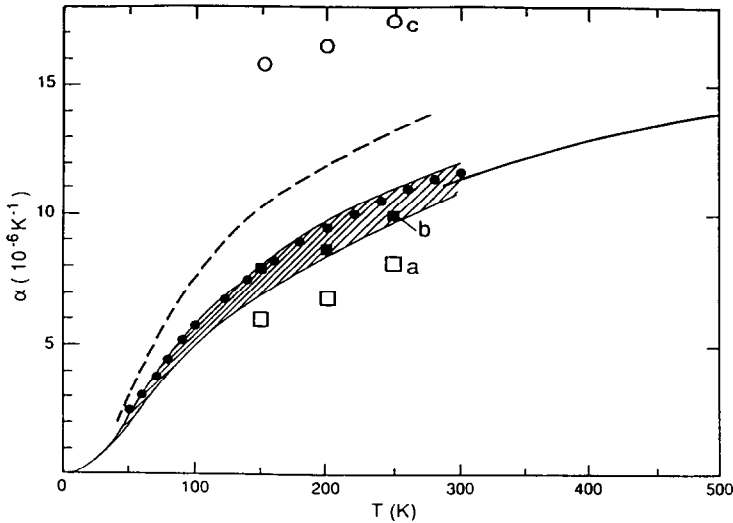

Fig. 9. Coefficients of thermal expansion of $Ba_2YCu_3O_7$ below 300 K. The figure is from ref. 5 and uses data from: ●, ref. 28, — — —, ref. 27; lattice parameters a, b and c, ref. 30; and ———, ref. 29. Measurements by dilatometry and XRD.

continuously during the transition from the orthorhombic to the tetragonal structure which occurs near 635°C in air. It is therefore concluded that this phase transition is second order. Also noted is the fact that the increase in the c lattice parameter contributes most to the expansion. The large compositional expansion between 450°C and 650°C is understood to be caused primarily by the loss of an oxygen atom from the 1-2-3 unit cell.

At temperatures below 300°C the structure can not change its oxygen content and normal thermal expansion and/or phase transitions are the source of any length changes. Figure 9 summarizes the changes in CTE between 5 K and 300 K for samples measured with capacitance dilatometry [25–27] and X-ray diffraction [28]. With the exception of one study [25] agreement on the magnitude of the CTE is good. Likewise only one of these studies could observe any anomaly in CTE at the 90 K T_c [26].

BiSrCaCu oxides

As has been discussed the Bi–Sr–Ca–Cu oxides do not densify easily unless Pb is added. Similarly, there is only a small variation in oxygen content with temperature, i.e. $\Delta x \approx 0.05$, as contrasted to $\Delta x \approx 0.8$ for 1-2-3. Thus the expansion data for this material are expected to be neither extensive nor unusual. White and co-workers have reported dilatometric data for a wide range of temperatures (1.0 K to 900 K) for several compositions [27]. Figure 10 shows the CTE for $Bi_{2.1}Sr_2CaCu_2O_x$ and $Bi_{1.6}Pb_{0.4}Sr_2Ca_{2.5}Cu_{3.5}O_x$ compared with that for 1-2-3. As expected the compositional effect causes a strong increase in expansion coefficient above
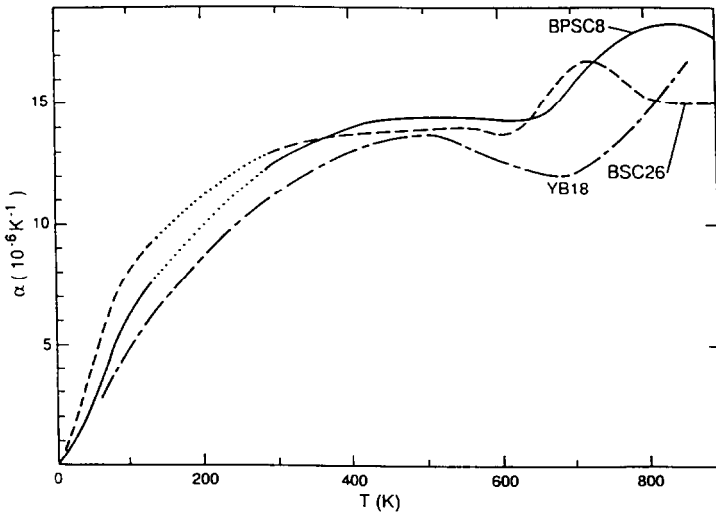

Fig. 10. Coefficients of thermal expansion between 5 K and 900K for $Bi_{2.1}Sr_2CaCu_2O_8$ (BSC26), $Bi_{1.6}Pb_{0.4}Sr_2Ca_{2.5}Cu_{3.5}O_8$ (BPSC8) and $Ba_2YCu_3O_7$ (YB18). Measurements by mechanical dilatometry in air.
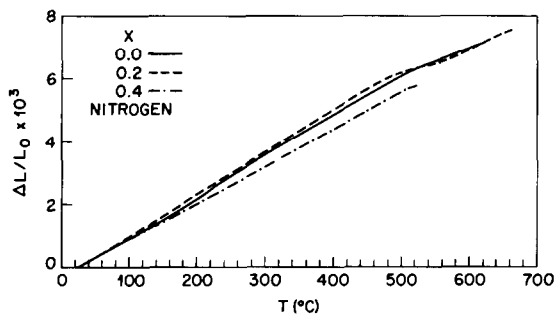
Fig. 11. Expansion of $Pb_2Sr_2(Y_{1-x}Ca_x)Cu_3O_8$ in nitrogen. Heating rate $4\,^\circ C$ min^{-1}.

$450\,^\circ C$ (723 K) for 1-2-3 while the CTE values for the Bi materials remain less than $20 \times 10^{-6}\,^\circ C^{-1}$. Interesting are the small changes in CTE, which are observed above $350\,^\circ C$ for the Bi compounds. By analogy to 1-2-3 a relation between the change in CTE and a variation in oxygen is suspected. A dilatometric study has related linear shrinkage to oxygen loss in Bi_2Sr_2 $Ca_{0.9}Y_{0.1}Cu_2O_{8+\delta}$ [29]. At $600\,^\circ C$ at length change of -0.25% results from $\Delta\delta = -0.04$.

$Pb_2Sr_2(YCa)Cu_3O_8$

This compound family has a structure similar to 1-2-3 but contains an arrangement of in addition double pyramidal planes (PbO_5–CuO_δ–PbO_5) at the center of the unit cell [30]. As in the case of 1-2-3 the expansion behavior of the PbSr family is a combination of compositional and thermal effects where x is defined as $Pb_2Sr_2Y_{1-x}Ca_xCu_3O_8$ [31]. In the absence of oxygen the thermal expansions for $x = 0, 0.2$ and 0.4 appear normal with little effect of Ca content (Fig. 11). In oxygen, however, an anomalously large expansion begins at $300\,^\circ C$ and a strong effect of Ca content is seen (Fig. 12). The expansion shows two maxima of about 1.4% near $550\,^\circ C$ and $700\,^\circ C$. The
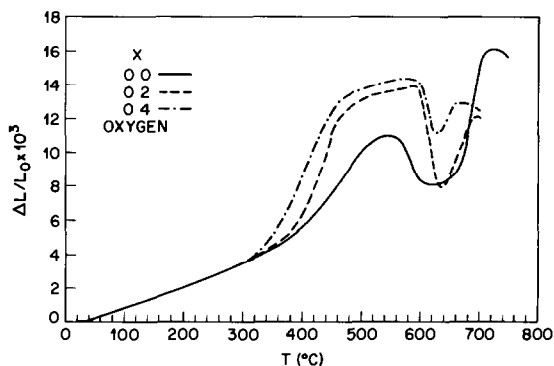

Fig. 12. Expansion of $Pb_2Sr_2(Y_{1-x}Ca_x)Cu_3O_8$ in oxygen. Heating rate $4\,^\circ C$ min^{-1}.
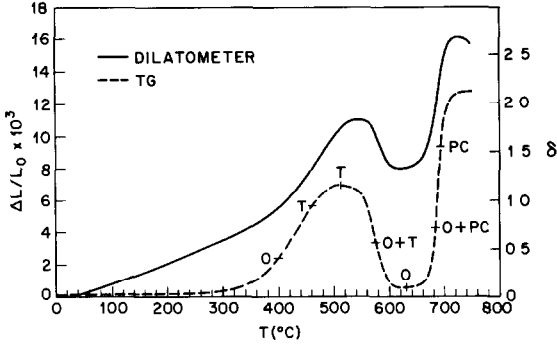
Fig. 13. Thermal expansion and TG curves for $Pb_2Sr_2YCu_3O_8$ in oxygen; heating rate $4°C$ min^{-1}.

compositional component of this expansion is seen by matching the temperature dependence of the dilatometric and TG data (Fig. 13). A gain or loss of oxygen is mimicked by an increase or decrease in length. There is a significant difference between $Pb_2Sr_2YCu_3O_8$ and 1-2-3, and this is seen in the opposite sense of the compositional expansion as the oxygen content of the atmosphere is changed isothermally (Fig. 14). It has been suggested that the expansion of the $Pb_2Sr_2(YCa)Cu_3O_8$ unit cell with oxygen addition is related to a relaxation of the vertical bonds between the central plane Cu and oxygen which lie between the PbO_5 pyramids. When oxygen is added to 1-2-3, the Cu atoms adjacent to the inserted oxygen are not shielded and increase their coupling with oxygen in CuO_5 pyramids. Hence the lattice of 1-2-3 shrinks on oxidation.
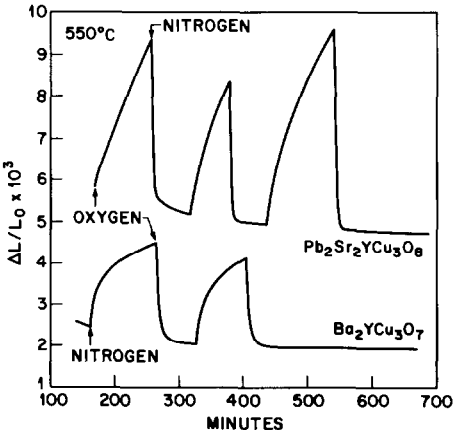

Fig. 14. Isothermal expansion of $Pb_2Sr_2YCu_3O_8$ and $Ba_2YCu_3O_8$ as the atmosphere is switched between oxygen and nitrogen at $550°C$. Measurements by dilatometry.

CONCLUSIONS

In summary HTSC materials show many interesting anomalies in their expansion behavior. By combining the expansion measurements with compositional determinations such as TG, it is possible to distinguish between the compositional and thermal contributions. The expansion responses to oxygen addition are unique for each oxide. Shrinkage is found for $Ba_2YCu_3O_{6.2}$ + oxygen while enlargement is found for $Pr_2Sr_2(YCa)Cu_3O_8$ + oxygen.

REFERENCES

1 M.F. Yan, H.C. Ling, H.M. O'Bryan, P.K. Gallagher and W.W. Rhodes, Mater., Sci. Eng. B, 1 (1988) 119.
2 D.R. Clarke, T.M. Shaw and D. Dimos, J. Am. Ceram. Soc., 72 (1989) 1103.
3 S. Jin, T.H. Tiefel, R.E. Sherwood, M.E. Davis, R.B. van Dover, G.W. Kamlott, R.A. Fastnocht and H.D. Keith, Phys. Rev. B, 37 (1988) 7850.
4 Y. Ibara, H. Nasu, T. Imura and Y. Osaka, Jpn. J. Appl. Phys., 28 (1989) L37.
5 G. Grader, H.M. O'Bryan and W.W. Rhodes, Appl. Phys. Lett., 52 (1988) 1831.
6 H. Maeda, Y. Tanaka, M. Fukutomi and T. Asano, Jpn. J. Appl. Phys., 27 (1988) L209.
7 D.W. Johnson and W.W. Rhodes, J. Am. Ceram. Soc., 72 (1989) 2346.
8 R. Tripathi, personal communication.
9 T. Asano, Y. Tanaka, M. Fukutomi, K. Jikihara, J. Machida and H. Maeda, Jpn. J. Appl. Phys., 27 (1988) L1652.
10 Y. Tanaka, T. Asano, K. Jikihura, M. Fukutomi, J. Machida and H. Maeda, Jpn. J. Appl. Phys., 27 (1988) L1655.
11 N. Murayama, E. Sudo, M. Awano, K. Kani and Y. Torii, Jpn. J. Appl. Phys., 27 (1988) L1856.
12 U. Endo, S. Koyama and T. Kawai, Jpn. J. Appl. Phys., 27 (1988) L1476.
13 T. Komatsu, R. Sato, C. Hirose, K. Matsuita and T. Yamashita, Jpn. J. Appl. Phys., 27 (1988) L2293.
14 M. Takano, J. Takada, K. Oda, H. Kitaquchi, Y. Miura, Y. Ikada, Y. Tomii and H. Mazaki, Jpn. J. Appl. Phys., 27 (1988) L1041.
15 S. Adachi, H. Hirano, Y. Takahashi, O. Inove and S. Kawashima, Jpn. J. Appl. Phys., 28 (1989) L209.
16 H. Nobumasa, K. Shimizu, Y. Kitano and T. Kawai, Jpn. J. Appl. Phys., 27 (1988) L846.
17 K. Imai and H. Matsuoba, preprint of paper presented at Workshop on HTSC, Huntsville, AL, May 1989.
18 R.G. Buckley, J.L. Tallon, I.W.M. Brown, M.R. Presland, N.E. Flower, P.W. Grilberd, M. Bowden and N.B. Milestone, Physica C, 156 (1988) 629.
19 D.E. Morris, C.T. Hultgren, A.M. Markelz, J.Y.T. Wei, N.G. Asmar and J.H. Nickel, Phys. Rev. B, 39 (1989) 6612.
20 P.K. Gallagher, H.M. O'Bryan, S.A. Sunshine and D.W. Murphy, Mater. Res. Bull., 22 (1987) 995.
21 H.M. O'Bryan and P.K. Gallagher, Adv. Ceram. Mater., 2 (3B) (1987) 640.
22 K. Yukino, T. Sato, S. Doba, F.P. Okamura and A. Ono, Jpn. J. Appl. Phys., 26 (1987) L869.
23 H.M. O'Bryan and P.K. Gallagher, J. Mater. Res., 3 (1988) 619.

24 J.D. Jorgensen, M.A. Beno, D.G. Hinks, L. Soderholm, K.J. Volin, R.,L. Hitterman, J.D. Grace and I.K. Schuller, Phys. Rev. B, 36 (1987) 3608.

25 E. du Tremolet, B. Barbara and J.H. Henry, J. Magn. Magn. Mater. 71 (1988) L125.

26 M. Lang, T. Lechner, S. Riegel, F. Steglich, G. Weber, T.J. Kim, B. Lüthi, B. Wolf, H. Rietschel and M. Wilhelm, J. Phys. Condensed Matter B, 69 (1988) 459.

27 G.K. White, S.J. Collocott, R. Driver, R.B. Roberts and A.M. Stewart, J. Phys. C, 21 (1988) L631.

28 H. You, J.D. Axe, X.B. Kan, S. Hashimoto, S.C. Moss, J.Z. Liv, G.W. Crabtree and D.J. Kam, Phys. Rev. B, 38 (1988) 9213.

29 W.A. Groen and D.M. de Leeuw, Physica C, 159 (1989) 417.

30 R.J. Cava, B. Batlogg, J. J. Krajewski, L.W. Rupp, L.F. Schneemeyer, T. Siegrist, R.B. van Dover, P. Marsh, W.F. Peck, Jr, P.K. Gallagher, S.H. Glarum, J.H. Marshall, R.C. Farrow, J.V. Waszczak, R. Hull and P. Trevor, Nature, 336 (1988) 211.

31 H.M. O'Bryan and P.K. Gallagher, Chem. Mater., 1 (1989) 526.